J. Am. Chem. Soc. **1990**, *112*, 8645-8649

Inclusion and Stabilization of Electrochemically Generated Anion Radicals of Dicyanobenzenes by Cyclodextrins in Water

Kenji Kano,* Kazuya Mori, Bunji Uno, Masashi Goto, and Tanekazu Kubota

Contribution from Gifu Pharmaceutical University, 5-6-1 Mitahora-higashi, Gifu 502, Japan.
Received May 14, 1990

Abstract: The interaction between cyclodextrins (CyDs) (α-, β-, γ-, and 2,6-*O*-dimethyl-β-CyDs) and the electrogenerated-intermediate anion radicals of 1,2- (PN), 1,4- (TPN), and 1,3-dicyanobenzenes in aqueous solution has been investigated by cyclic voltammetry and in situ electrochemical electron spin resonance (ESR) spectroscopy. Most strikingly, the addition of 2,6-*O*-dimethyl-β-CyD (DMβ-CyD) changes an irreversible two-electron-reduction wave of PN or TPN to a reversible one-electron wave, yielding its stable anion radical ($PN^{\bullet -}$ or $TPN^{\bullet -}$), at a slow scan rate. The cyclic voltammetric and absorption spectral data have revealed a 1:1 inclusion complex formation of CyDs with the anion radicals as well as with the parent dicyanobenzenes, where the anion radicals are included more tightly than the parents and stabilized in a microscopic environment of the CyD cavity with respect to the consumptive homogeneous chemical reaction. Digital simulation analysis of the voltammograms points to the relatively aprotic property of the CyD cavity. The ESR spectral behavior of $PN^{\bullet -}$ and $TPN^{\bullet -}$ in the presence of DMβ-CyD indicates that $PN^{\bullet -}$ penetrates the cavity with its benzene ring first at the 3-hydroxyl side of the CyD and $TPN^{\bullet -}$ penetrates the cavity with its cyano group first. The unusual stronger inclusion of the anion radicals can be explained in terms of their dipole–induced dipole interaction. The dependence of the formation constants on the dicyanobenzene isomers and the CyDs is interpreted in view of the steric specificity.

Cyclodextrins (CyDs), torus-shaped cyclic oligosaccharides, are known to have unique characteristics of molecular recognition and hydrolase-like catalysis.[1] Thus, interest in the mechanism of their molecular recognition[1] and in a variety of their applications such as enzyme or receptor models,[1] drug delivery systems,[2] and analytical chemistry[3] has grown considerably. With respect to reactions of organic guest molecules in such CyD systems, the interaction of CyDs with the parent guest molecules appears to have been emphasized. Actually, no such studies on the interaction between CyDs and unstable intermediates or intermediate radicals have been reported, although the inclusion of stable neutral radicals by CyDs is known.[4,5] In contrast to the CyD systems, the marked stabilization of reaction-intermediate radicals has been demonstrated in micelle + substrate systems,[6] which have characteristics similar to those of the CyD systems.[7] In light of the relatively hydrophobic nature of the CyD cavity,[1] the reaction-intermediate radicals must be stabilized in the CyD systems if the CyD includes the radicals. However, one question arises: Why can radicals be incorporated into the hydrophobic cavity, when they are charged?

Recently, we have reported the voltammetric behavior of *p*-nitrophenolate anion (p-NP$^-$) in the presence of α-CyD and have shown that its one-electron-reduced divalent anion radical (p-NP$^{\bullet 2-}$) is also incorporated into the α-CyD cavity, although the formation constant is 125 times smaller than that of the p-NP$^-$–α-CyD complex.[8] The decrease in affinity by the reduction of p-NP$^-$ is attributable to the increase in the negative charge of the guest molecule, as in the case of benzoate anion–α-CyD complex: benzoate binds 82 times more loosely with α-CyD than benzoic acid.[9]

In this paper, we investigate the redox reactions of dicyanobenzene + CyD systems in aqueous solution as model reactions of CyD systems, paying attention to the nature of the interaction between CyDs and the electrogenerated anion radicals of dicyanobenzenes. The unstable radicals in the absence and presence of CyD have been successfully detected in aqueous media by (fast-scan) cyclic voltammetry and in situ electrochemical electron spin resonance (ESR) spectroscopy. The results have indicated a 1:1 complex formation of the electrogenerated anion radicals as well as the parent guest molecules with CyDs, resulting in enhanced stabilization of the radicals, in which the anion radical binds more strongly in the CyD cavity than the parent molecules. The unusual stronger inclusion of the anion radicals can be interpreted in terms of their dipole–induced dipole interaction.

Experimental Section

Materials. 2,6-*O*-Dimethyl-β-cyclodextrin (DMβ-CyD), α-CyD, β-CyD, and γ-CyD were purchased from Wako (Japan) and purified by recrystallization from methanol, a 1-propanol + water mixture, water, and a 1-propanol + water mixture, respectively, with the crystals being dried over diphosphorus pentoxide under vacuum. Phthalonitrile (PN; 1,2-dicyanobenzene), terephthalonitrile (TPN; 1,4-dicyanobenzene), and isophthalonitrile (IPN; 1,3-dicyanobenzene), obtained from Wako, were recrystallized from an ethanol + water mixture, ethanol, and ethanol, respectively. Tetraethylammonium bromide (TEAB; Wako) was re-

---

(1) For reviews, see: (a) Bender, M. L.; Komiyama, M. *Cyclodextrin Chemistry*; Springer: New York, 1978. (b) Saenger, W. *Angew. Chem., Int. Ed. Engl.* **1980**, *19*, 344. (c) Breslow, R. *Adv. Chem. Ser.* **1980**, *91*, 1. (d) Tabushi, I. *Acc. Chem. Res.* **1982**, *15*, 66. (e) Atwood, J. L., Davies, J. E. D., MacNicol, D. D., Eds. *Inclusion Compounds*; Academic Press: London, 1984; Vols. 2, 3. (f) Matsui, Y. *Hyomen* **1986**, *24*, 332. (g) Diederich, F. *Agnew. Chem., Int. Ed. Engl.* **1988**, *27*, 362.

(2) (a) Uekama, K.; Otagiri, M. *CRC Crit. Rev. Ther. Drug Carrier Syst.* **1987**, *3*, 1. (b) Duchene, D.; Glomot, F.; Vaution, C. *Cyclodextrins - Their Industrial Uses*; Duchene, D., Ed.; Ed. Sante: Paris, 1987; pp 211-257. (c) Ukekama, K.; Irie, T., pp 393-439 in ref. 2b.

(3) (a) Szejtli, J.; Zsadon, B.; Cserhati, T. *Ordered Media in Chemical Separations*; Hinze, W. L., Armstrong, D. W., Eds.; American Chemical Society: Washington, DC, 1987; Chapter 11. (b) Armstrong, D. W. *Anal. Chem.* **1987**, *59*, 84A. (c) Armstrong, D. W. *Sep. Purif. Methods* **1985**, *14*, 213. (d) Bello, J. M.; Hurtubise, R. J. *Anal. Chem.* **1988**, *60*, 1285, 1291. (e) Alak, A. M.; Vo-Dinh, T. *Anal. Chem.* **1988**, *60*, 596. (f) Matsue, T.; Fijihira, M.; Osa, T. *Anal. Chem.* **1981**, *53*, 722. (g) Matsue, T.; Akiba, U.; Osa, T. *Anal. Chem.* **1986**, *58*, 2096. (g) Blyshak, L. A.; Rossi, T. M.; Potonay, G.; Warner, I. M. *Anal. Chem.* **1988**, *60*, 2127.

(4) (a) Kotake, Y.; Janzen, E. G. *J. Am. Chem. Soc.* **1988**, *110*, 3699. (b) Kotake, Y.; Janzen, E. G. *Chem. Phys. Lett.* **1988**, *150*, 199. (c) Janzen, E. G.; Kotake, Y. *J. Am. Chem. Soc.* **1988**, *110*, 7912. (d) Kotake, Y.; Janzen, E. G. *J. Am. Chem. Soc.* **1989**, *111*, 2066. (e) Kotake, Y.; Janzen, E. G. *J. Am. Chem. Soc.* **1989**, *111*, 7319. (f) Paton, R. M.; Kaiser, E. T. *J. Am. Chem. Soc.* **1970**, *92*, 4723. (g) Flohr, K.; Paton, R. M.; Kaiser, E. T. *Chem. Commun.* **1971**, 1621. (h) Atherton, N. M.; Strach, S. J. *J. Chem. Soc., Faraday Trans. I* **1975**, *71*, 357. (i) Atherton, N. M.; Strach, S. J. *J. Magn. Reson.* **1975**, *17*, 134. (j) Martinie, J.; Michon, J.; Rassat, A. *J. Am. Chem. Soc.* **1975**, *97*, 1818.

(5) (a) Flohr, K.; Paton, R. M.; Kaiser, E. T. *J. Am. Chem. Soc.* **1975**, *97*, 1209. (b) Okazaki, M.; Kuwata, K. *J. Phys. Chem.* **1984**, *88*, 4181. (c) Kubozono, Y.; Ata, M.; Aoyagi, M.; Gondo, Y. *Chem. Phys. Lett.* **1987**, *137*, 467.

(6) (a) McIntire, G. L.; Chiappardi, D. M.; Casselberry, R. L.; Blout, H. N. *J. Phys. Chem.* **1982**, *86*, 2632. (b) McIntire, G. L.; Blount, H. N. *J. Am. Chem. Soc.* **1979**, *101*, 7720. (c) Meyer, G.; Nadjo, L.; Savêant, J. M. *J. Electroanal. Chem.* **1981**, *119*, 417.

(7) Fendler, J. H.; Fendler, E. J. *Catalysis in Micellar and Macromolecular Systems*; Academic Press: New York, 1975.

(8) Kano, K; Mori, K.; Uno, B.; Kubota, T. *J. Electroanal. Chem.* **1990**, *283*, 187.

(9) Bergeron, R. J.; Channing, M. A.; McGovern, K. A. *J. Am. Chem. Soc.* **1978**, *100*, 2878.

0002-7863/90/1512-8645$02.50/0 © 1990 American Chemical Society

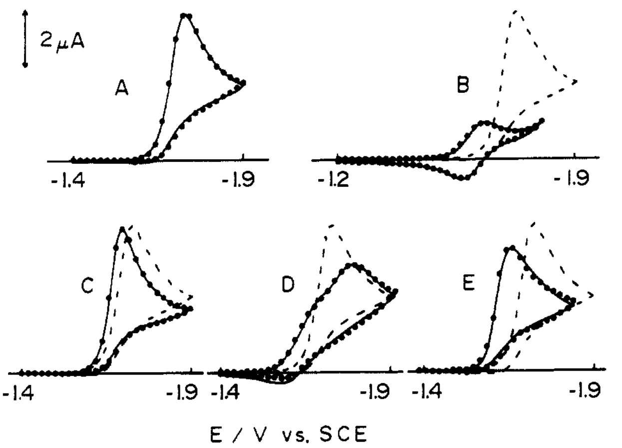

Figure 1. Cyclic voltammograms of 3.18×10^{-4} M PN at $v = 0.1$ V s^{-1} in the absence (A and ---) and in the presence of (B) 0.05 M DMβ-CyD, (C) 0.05 M α-CyD, (D) 0.01 M β-CyD, and (E) 0.05 M γ-CyD in water containing 0.2 M TEAB (●). (—) Regression curves obtained by the digital simulation + curve-fitting analysis (see text).

crystallized from acetonitrile and used as a supporting electrolyte for aqueous electrolysis solution. Tetrapropylammonium perchlorate (TPAP) was prepared as described previously[10] and used as a supporting electrolyte for *N*,*N*-dimethylformamide (DMF). Triply distilled water was used. DMF was carefully purified as reported in a previous paper.[10]

Electrochemical Measurements. Cyclic voltammetry was performed at 25.0 ± 0.1 °C with a three-electrode system consisting of a Metrohm EA-290 hanging mercury drop electrode (HMDE), a platinum wire counter electrode, and a saturated calomel reference electrode (SCE). The surface area of the HMDE was 0.0187 ± 0.0003 cm^2 at a scan rate (v) ≤ 0.5 V s^{-1} and 0.0090 ± 0.0003 cm^2 at $v > 0.5$ V s^{-1}. The other details of the electrochemical measurements were described in a previous paper.[8]

Digital Simulation of the Voltammogram. The digital simulation of the cyclic voltammogram was carried out on the basis of the following mechanism involving two sequential one-electron transfers:

$$A \underset{E_1}{\overset{e^-}{\rightleftharpoons}} B \underset{E_2}{\overset{e^-}{\rightleftharpoons}} C \xrightarrow[\text{fast}]{} D \qquad (1)$$

The redox potential of the second electron transfer (E_2) as well as the electron-transfer rate constant and the transfer coefficient of each electron transfer step was adjusted to give the best fit to the voltammogram by the nonlinear least-squares method. The redox potential of the first electron transfer (E_1) was evaluated experimentally and used as a fixed parameter. The spherical diffusion effect on the voltammogram was also taken into consideration.[11,12] The other procedure of the digital simulation + curve-fitting analysis of cyclic voltammograms has been described in previous papers.[11,13]

Spectroscopic Measurements. All absorption spectroscopic measurements (at 25.0 ± 0.1 °C) have been described elsewhere.[14] In situ electrochemical ESR spectroscopy was performed as reported in previous papers.[8,15] Controlled-potential electrolysis was performed at room temperature with a mercury pool electrode as the working electrode. An internal flow method developed in this laboratory[15] was adopted for in situ ESR measurements of unstable intermediate free radicals. Details of the ESR simulations and the determinations of the ESR spectral parameters were described in previous papers.[8,15]

Results and Discussion

Cyclic Voltammetry in PN + CyD Systems. Typical cyclic voltammograms of PN in the absence and presence of DMβ-, α-, β-, and γ-CyDs at $v = 0.1$ V s^{-1} are illustrated in Figure 1. In the absence of CyD, PN gave an irreversible two-electron-reduction wave. The addition of the CyDs caused drastic changes in the cyclic voltammogram. The addition of DMβ-CyD changed the irreversible wave of PN to a reversible one-electron redox wave, yielding its anion radical (PN$^{\bullet-}$). On addition of β-CyD, the irreversible wave became two merged irreversible waves. These results point to the stabilization of the PN$^{\bullet-}$ intermediate by the CyDs, especially by DMβ- or β-CyD.

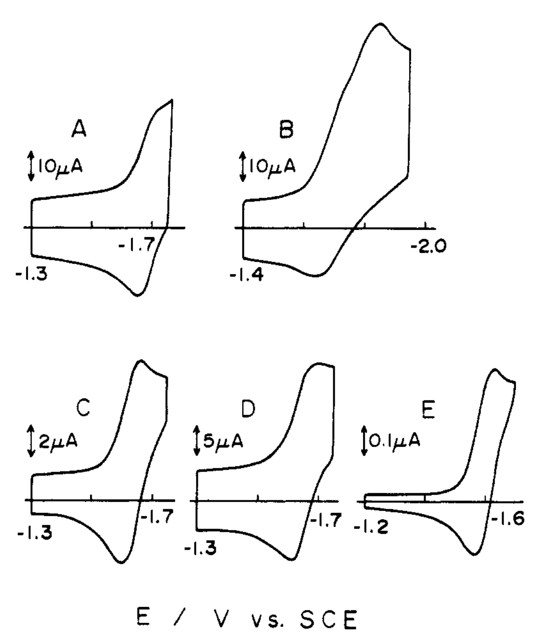

Figure 2. Cyclic voltammograms of 3.18×10^{-4} M PN in the absence (A) and in the presence of (B) 0.05 M α-CyD, (C) 0.01 M β-CyD, (D) 0.05 M γ-CyD, and (E) 0.05 M DMβ-CyD. v (V s^{-1}): (A) 122, (B) 120, (C) 12, (D) 60, (E) 0.02.

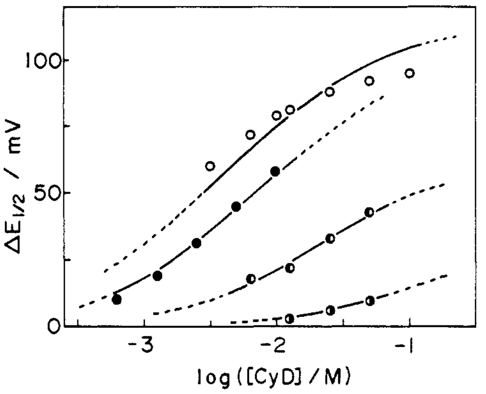

Figure 3. Dependences of $\Delta E_{1/2}$ ($=E_{1/2,\mathrm{app}} - E_{1/2}$) values on the concentrations of various CyDs: (○) DMβ-CyD; (●) β-CyD; (◐) γ-CyD; (◑) α-CyD. $E_{1/2} = -1.690$ V vs SCE. Curves represent the regression curves analyzed on the basis of eq 3.

The stabilization was also confirmed by fast-scan cyclic voltammetry as shown in Figure 2: quasi-reversible waves appeared in the presence of 0.01 M β-CyD and 0.05 M γ-CyD at $v = 12$ and 60 V s^{-1}, respectively, while in the absence of the CyD such a quasi-reversible wave appeared at v near 150 V s^{-1}. In the presence of 0.05 M DMβ-CyD, the voltammogram retained reversible characteristics even at $v = 0.02$ V s^{-1}. The apparent half-wave potential ($E_{1/2,\mathrm{app}}$), taken as the midpoint between the cathodic and anodic peak potentials, continued to shift in the positive direction with the increase in the CyD concentrations ([CyD]), as shown in Figure 3, where $\Delta E_{1/2}$ is defined as $\Delta E_{1/2} = E_{1/2,\mathrm{app}} - E_{1/2}$, $E_{1/2}$ being the half-wave potential in the absence of CyD and estimated to be -1.690 V vs SCE. This implies that the PN$^{\bullet-}$ *anion* is bound more strongly to the CyDs than the neutral PN.

Absorption Spectroscopy in PN + CyD Systems. The UV absorption spectrum of PN changed with the change in [CyD]:

---

[10] Kubota, T.; Kano, K.; Uno, B.; Konse, T. *Bull. Chem. Soc. Jpn.* **1987**, *60*, 3865.

[11] Kano, K.; Mori, K.; Uno, B.; Kubota, T.; Ikeda, T.; Senda, M. *Bioelectrochem. Bioenerg.* **1990**, *23*, 227.

[12] Feldberg, S. W. *Electroanalytical Chemistry*; Bard, A. J., Ed.; Marcel Dekker: New York, 1969; Vol. 3, p 200.

[13] Kano, K.; Konse, T.; Uno, B.; Kubota, T. *Redox Chemistry and Interfacial Behavior of Biological Molecules*; Dryhurst, G., Niki, K., Eds.; Prenum Press: New York, 1987; p 267.

[14] Uno, B.; Kaida, N.; Kawakita, T.; Kano, K.; Kubota, T. *Chem. Pharm. Bull.* **1988**, *36*, 3753.

[15] Kano, K.; Mori, K.; Konse, T.; Uno, B.; Kubota, T. *Anal. Sci.* **1989**, *5*, 651.

Table I. Formation Constants of Dicyanobenzene–CyD and Dicyanobenzene Anion Radical–CyD Complexes in Water Containing 0.2 M TEAB at 25 °C

		host			
guest	K (M^{-1})	α-CyD	β-CyD	γ-CyD	DMβ-CyD
PN	K_{ox}	7.6 ± 2.0	29.7 ± 1.3	25.0 ± 1.4	50.3 ± 3.0
$PN^{\bullet -}$	K_{red}	26.0 ± 0.6	1714 ± 83	287 ± 14	4210 ± 440
TPN	K_{ox}	17.9 ± 1.8	10.4 ± 2.0	*a*	12.2 ± 1.9
$TPN^{\bullet -}$	K_{red}	814 ± 102	2140 ± 103	*a*	9030 ± 1230

[a] Estimation failed (see text).

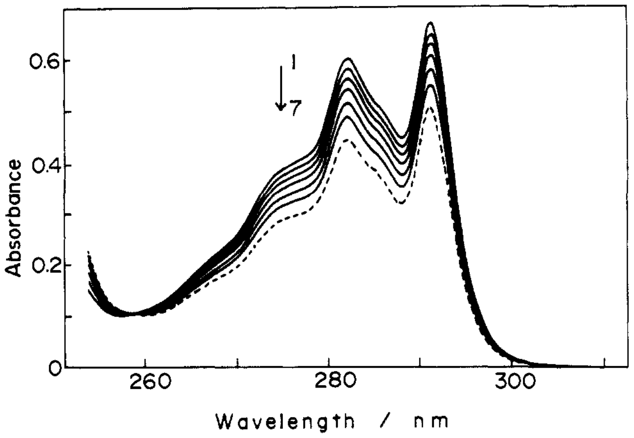

Figure 4. Absorption spectra of 3.18 × 10^{-4} M PN at various concentrations of DMβ-CyD in water containing 0.2 M TEAB at a light path length of 1.0 cm. [DMβ-CyD] (10^{-2} M): (1) 0, (2) 0.313, (3) 0.625, (4) 1.25, (5) 2.50, (6) 5.00. Curve 7 (---) is the PN–DMβ-CyD complex itself, calculated from K_{ox}.

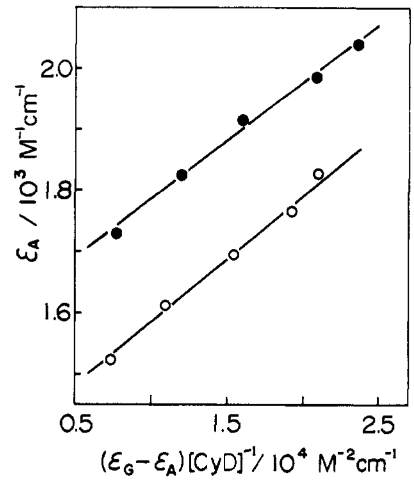

Figure 5. Linear relations of ϵ_A values to $(\epsilon_G - \epsilon_A)[CyD]^{-1}$ values at (●) 291 and (○) 282 nm for PN + DMβ-CyD system.

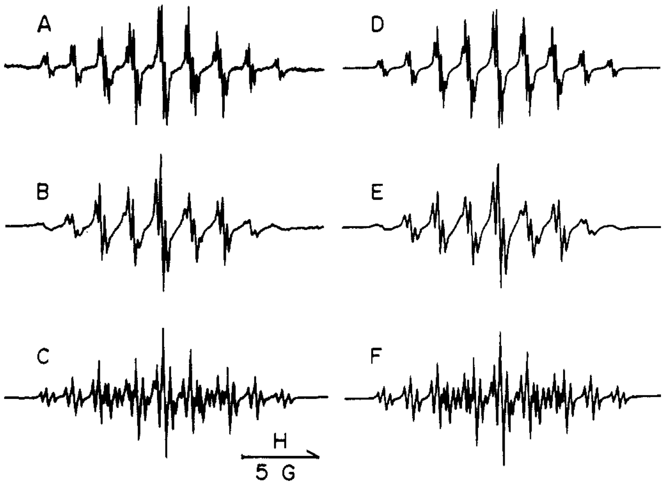

Figure 6. ESR spectra of $PN^{\bullet -}$ in (A) water + ethanol (5% v/v) containing 0.5 M TEAB, (B) 0.05 M DMβ-CyD + (A), and (C) DMF containing 0.15 M TPAP. The mercury working electrode potentials were as follows: (A) −1.70, (B) −1.65, and (C) −1.70 V vs SCE. PN (M): (A) 2.00 × 10^{-3}, (B) 2.00 × 10^{-3}, (C) 5.31 × 10^{-4}. Simulated Lorentzian spectra (D–F), corresponding to spectra A–C in turn, were generated with the hfs constants and the line widths given in Table II.

the absorbance of PN in the 270–300-nm region (^1L_b band) decreased with increasing the [CyD] with an isosbestic point around 260 nm. An example is given in Figure 4 for the PN + DMβ-CyD system. This spectral behavior indicates a 1:1 inclusion complex (PN–CyD) formation from PN and the CyD. Under the conditions of the 1:1 inclusion complex formation equilibrium and of an excess of [CyD] compared with the total concentration of PN, the following equation can be derived[14,16]

$$\epsilon_A = (1/K_{ox})(\epsilon_G - \epsilon_A)/[CyD] + \epsilon_C \qquad (2)$$

where K_{ox} denotes the formation constant of the PN–CyD complex, defined as K_{ox} = [PN–CyD]/[PN][CyD], [PN] and [PN–CyD] being the concentrations of PN and PN–CyD. ϵ_G, ϵ_C, and ϵ_A represent the absorption coefficients of the free (PN) and complexed guests (PN–CyD) and the apparent one, respectively. Examples of the linear plots are given in Figure 5 for the data of Figure 4. The slope gave the K_{ox} value, which is summarized in Table I for each PN + CyD system. DMβ-CyD turned out to be the most suitable host for PN among the CyDs used.

Formation Constants of $PN^{\bullet -}$–CyD Complexes. Here, we tried to analyze the $\Delta E_{1/2}$ vs [CyD] relationships quantitatively, in order to evaluate the formation constants (K_{red}) of the inclusion complexes ($PN^{\bullet -}$–CyD) between $PN^{\bullet -}$ and the CyDs. When an equilibrium involving a 1:1 complex formation of $PN^{\bullet -}$ as well as PN by CyD and a one-electron redox reaction of PN and the PN–CyD complex are considered, the [CyD] dependence of $\Delta E_{1/2}$ is given by[8,17]

$$\frac{F\Delta E_{1/2}}{RT} = \ln\left(\frac{1 + K_{red}[CyD]}{1 + K_{ox}[CyD]}\right) + \frac{1}{2}\ln\left\{\frac{(1 + rK_{red}[CyD])(1 + K_{ox}[CyD])}{(1 + K_{red}[CyD])(1 + rK_{ox}[CyD])}\right\} \qquad (3)$$

where r is defined as $r = D_C/D_F$, D_C and D_F being the diffusion coefficients of PN (or $PN^{\bullet -}$) and the PN–CyD (or $PN^{\bullet -}$–CyD) complex. The r value was estimated according to the equation $r = (M_{PN}/M_{PN\text{-}CyD})^{1/2}$, M_{PN} and $M_{PN\text{-}CyD}$ being the molecular weights of PN and the PN–CyD complex, respectively.[18] Regression analyses of the $\Delta E_{1/2}$ vs [CyD] plots of eq 1, by use of the spectroscopically estimated K_{ox} values, yielded the K_{red} values, which are summarized in Table I. The solid lines in Figure 3 represent the resultant regression curves.

DMβ- and β-CyDs were found to be more suitable hosts for $PN^{\bullet -}$ and PN than γ- and α-CyDs, which can be interpreted in terms of the steric specificity of CyDs. The inner diameters of α-, β-, and γ-CyDs are 4.7–5.2, 6.0–6.4, and 7.5–8.3 Å, respec-

---

(16) (a) Kubota, T. *J. Am. Chem. Soc.* **1965**, *87*, 458. (b) Kubota, T. *J. Am. Chem. Soc.* **1966**, *88*, 211.

(17) Meites, L. *Polarographic Techniques*, 2nd ed.; John Wiley: New York, 1965; Chapter 5, pp 267–284.

(18) Martin, R. B. *Introduction to Biophysical Chemistry*; McGraw-Hill: New York, 1964; Chapter 9.

Table II. Hyperfine Splitting Constants and Line Widths from ESR Spectra of Dicyanobenzene Anion Radicals in Various Media at Room Temperature

radical	medium	α_N (G) N(1,2)	$\alpha_H{}^a$ (G) H(3,6)	$\alpha_H{}^a$ (G) H(4,5)	ΔH (G)
$PN^{\bullet-}$	water + 5% ethanol^b	1.81	0.20	3.82	0.13
$PN^{\bullet-}$	0.05 M DMβ-CyD + water + 5% ethanol^b	1.80	0.32	3.92	$0.17 - 0.03m + 0.05m^{2\,d}$
$PN^{\bullet-}$	DMF^c	1.74	0.40	4.11	0.12

radical	medium	α_N (G) N(1,4)	α_H (G) H(2,3,5,6)	ΔH (G)
$TPN^{\bullet-}$	water + 10% ethanol^b	1.85	1.68	0.11
$TPN^{\bullet-}$	0.06 M DMβ-CyD + water + 10% ethanol^b	1.89	1.63	$0.17 + 0.05m^{2\,d}$
$TPN^{\bullet-}$	DMF^c	1.80	1.59	0.12

^{a}Error is ±0.01 G (1 G = 1 × 10^{-4} T). ^{b}Containing 0.5 M TEAB. ^{c}Containing 0.15 M TPAP. ^{d}See eq 4.

tively.[1b] Thus, we predict that the γ- and α-CyD cavities appear to be too large and too small, respectively, for the PN or $PN^{\bullet-}$ guest. The result that DMβ-CyD is a more suitable host than β-CyD for PN and $PN^{\bullet-}$ might be due to the more hydrophobic nature of the former cavity than that of the latter.[2c,19] On the other hand, $PN^{\bullet-}$ was enclosed in the CyD cavity more strongly than PN, resulting in an enhanced stabilization of $PN^{\bullet-}$, with respect to the consumptive homogeneous chemical reaction.

ESR Spectroscopy of $PN^{\bullet-}$. The ESR spectra of the (unstable) $PN^{\bullet-}$ intermediate in the absence and presence of DMβ-CyD were successfully recorded by employing the in situ electrochemical ESR method, as shown in Figure 6. Ethanol (5% v/v) was added to an aqueous solution in order to increase the solubility of PN. For comparison, the ESR spectrum of $PN^{\bullet-}$ in DMF was also recorded. While the ESR spectra of the free $PN^{\bullet-}$ both in water and in DMF were reproduced by the isotropic Lorentzian simulation (Figure 6, parts D and F), spectrum B in the presence of DMβ-CyD exhibited an anisotropic hyperfine splitting (hfs) due to the ^{14}N nuclei. Most notably, the spectrum in the low and high fields was broadened. The appearance of the anisotropy is attributable to the suppression of the radical rotation by the complex formation with DMβ-CyD.[5,8] As shown in spectrum E of Figure 6, the anisotropic ESR spectrum was well simulated by taking into account the spin quantum number (m) dependence of the line width (ΔH)[20]

$$\Delta H = A + Bm + Cm^2 \tag{4}$$

where A, B, and C depend on the rotational correlation time (τ_c) and on the anisotropic g and hfs tensors of the radical. Here, the m values of $PN^{\bullet-}$ are +2, +1, 0, −1, and −2 from low to high field.[21] The estimation of τ_c failed because of the lack of data concerning the anisotropic hfs tensors of $PN^{\bullet-}$.

Table II summarizes the hfs constants of those spectra. It should be noted that, in the presence of DMβ-CyD, the hfs constants of the hydrogen nuclei (α_H) are intermediate between those in protic (water) and aprotic (DMF) media, but the hfs constant of the nitrogen nuclei (α_N) is close to that in the protic medium.[22,23] This means that $PN^{\bullet-}$ penetrates the cavity with the benzene ring first at the 3-hydroxyl side of DMβ-CyD and with the cyano groups pointing out into aqueous solution. Although the stronger inclusion of the $PN^{\bullet-}$ *anion* relative to the neutral PN might be unusual in view of the hydrophobic nature of the CyD cavity, the direction of the penetration and the charge of $PN^{\bullet-}$ seem to enhance a dipole–induced dipole interaction, as suggested for p-NP^{-}–α-CyD complex.[24]

Table III. Apparent Comproportionation Constants of $PN^{\bullet-}$ in Various Media

medium	$K_{com}{}^c$
water^a	5^d
0.05 M DMβ-CyD^a	$1.6 \times 10^{4\,d}$
0.05 M α-CyD^a	3^d
0.01 M β-CyD^a	$1.1 \times 10^{2\,d}$
0.05 M γ-CyD^a	1^d
DMF^b	$1.37 \times 10^{7\,e}$

^{a}Containing 0.2 M TEAB. ^{b}Containing 0.1 M TPAP. ^{c}See eq 5. ^{d}Error in the estimation of E_2 based on eq 1 is ±2–±5 mV.[27] ^{e}The first and second electron transfers are reversible at v = 0.1 V s^{-1}.

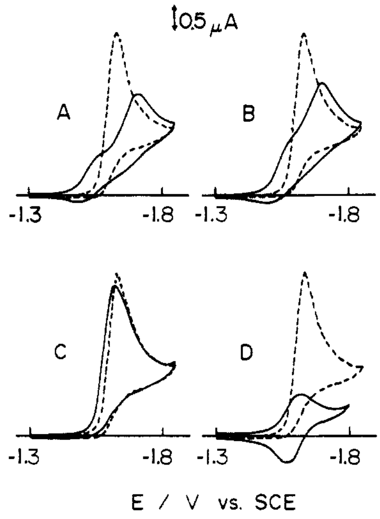

Figure 7. Cyclic voltammograms of 1.88 × 10^{-4} M TPN at v = 0.1 V s^{-1} in the absence (---) and the presence of (A) 0.05 M α-CyD, (B) 0.01 M β-CyD, (C) 0.05 M γ-CyD, and (D) 0.05 M DMβ-CyD (—) in water containing 0.2 M TEAB.

Stability of $PN^{\bullet-}$. The above results demonstrate that the $PN^{\bullet-}$ radical incorporated into the relatively hydrophobic cavity of CyDs is stabilized with respect to the consumptive homogeneous chemical reaction. Therefore, the estimation of the stability of $PN^{\bullet-}$ in the local microscopic environment is very important. We tried to evaluate the apparent comproportionation constant (K_{com}) of $PN^{\bullet-}$.[25] The digital simulation and curve-fitting analysis[26] allowed evaluation of the apparent redox potential of the second electron transfer (E_2), where we assume a simplified mechanism involving

---

(19) Miyamjima, K.; Mukai, T.; Nakagaki, M.; Otagiri, M.; Uekama, K. *Bull. Chem. Soc. Jpn.* **1986**, *59*, 643.

(20) (a) Kivelson, D. *J. Chem. Phys.* **1960**, *33*, 1094. (b) Wilson, R.; Kivelson, D. *J. Chem. Phys.* **1966**, *44*, 154.

(21) Gerson, F. *High Resolution E.S.R. Spectroscopy* (English Translation); Foerst, W., Grünewald, H., Eds.; John Wiley: New York, 1970; p 110.

(22) Such medium or solvent effects on hfs constants are well-known for aromtic nitro compounds: The α_N value increases with decreasing the water content of organic solvent + water mixtures.[23] This has been interpreted in terms of the redistribution of the π-electron charge and the spin density caused by localized solvent–radical ion complexes.[23]

(23) (a) Gendell, J.; Freed, J. H.; Fraenkel, G. K. *J. Chem. Phys.* **1962**, *37*, 452. (b) Ludwig, P.; Layloff, T.; Adams, R. N. *J. Am. Chem. Soc.* **1964**, *86*, 4568.

(24) Bergeron, R. J.; Channing, M. A.; Gibeily, G. J.; Pillor, D. M. *J. Am. Chem. Soc.* **1977**, *99*, 5146.

(25) The smallest value of v at which the (quasi) reversible one-electron redox wave can appear might be a qualitative parameter representing the stability of $PN^{\bullet-}$. However, it seems to be difficult to assess the value and also to interpret its physical meaning.

(26) The apparent diffusion coefficients (D_{app}) of the redox species A and B in eq 1 were estimated by $D_{app} = D_F(1 + rK[CyD]/(1 + K[CyD])$,[17] where K is K_{ox} and K_{red} for the species A and B, respectively, D_F and r being defined in text (see eq 3). Species C and D in eq 1 were assumed not to be included by CyD.

two sequential one-electron transfers, given by eq 1.[27] The experimental value of $E_{1/2,\mathrm{app}}$ (or $E_{1/2}$) was used as E_1 in eq 1. Some examples of the regression results are illustrated in Figure 1. Hence, the K_{com} value, defined as $K_{\mathrm{com}} = [\mathrm{B}]^2/([\mathrm{A}][\mathrm{C}])$, is evaluated by[28]

$$K_{\mathrm{com}} = \exp[(F/RT)(E_1 - E_2)] \qquad (5)$$

The estimated values of K_{com} in various media are summarized in Table III. DMβ-CyD was found to provide a relatively aprotic microscopic environment for $PN^{\bullet-}$: the K_{com} value is intermediate between those in water and in DMF. The K_{com} values appear to bear a parallel relationship to the K_{red} values, if the error in the estimation of E_2 and, hence, the K_{com} is taken into account.[27] The partial inclusion into the α-CyD cavity and the loose inclusion into the γ-CyD cavity of $PN^{\bullet-}$ would be responsible for the disappearance of the inherent aprotic nature of the CyD cavities. The more or less aprotic microscopic environment would prevent $PN^{\bullet-}$ from being protonated.

TPN + CyD Systems. In the previous section, we have interpreted the dependence of K_{ox} and K_{red} on the CyD species in terms of the dimensions of the cavities. This consideration led us to investigate the inclusion behavior of the other isomers of dicyanobenzenes and to compare it with that of PN (or $PN^{\bullet-}$).

Figure 7 shows cyclic voltammograms of TPN in the absence and presence of CyDs. As in the case of PN, the addition of DMβ-CyD changed an irreversible two-electron-reduction wave of TPN to a reversible one-electron redox wave, yielding its stable anion radical ($TPN^{\bullet-}$), at a slow v. In contrast with the PN + CyD systems, however, the addition of α-CyD to a TPN solution caused a split in the irreversible wave, resulting in a wave similar to that in the presence of β-CyD, while only few changes were observed by the addition of γ-CyD. These results are reasonable in view of the steric specificity of CyDs: α-CyD should be a more suitable host for TPN than γ-CyD, if TPN penetrates the cavity with one cyano group first at the 3-hydroxyl side (see the following text).

The formation constants of the TPN–CyD and $TPN^{\bullet-}$–CyD complexes were evaluated by cyclic voltammetry and spectroscopy, in a way similar to that described above. The results are also summarized in Table I. It is noteworthy that the values of the ratio $K_{\mathrm{red}}/K_{\mathrm{ox}}$ in the TPN + CyD systems are larger than those in the PN + CyD systems. The spectral change in the TPN + γ-CyD system was too small to evaluate K_{ox}, and, hence, the evaluation of K_{red} failed. We can presume that the values of K_{ox} and K_{red} for the TPN + γ-CyD system are much smaller than those for the TPN + α-CyD system.

As in the case of $PN^{\bullet-}$, in situ electrochemical ESR spectral measurements of $TPN^{\bullet-}$ in various media provided confirming evidence for the $TPN^{\bullet-}$–CyD complex formation: the ESR spectrum of $TPN^{\bullet-}$ in the presence of DMβ-CyD exhibited an anisotropic hfs due to the ^{14}N nuclei, while the spectra both in aqueous and in DMF solution were isotropic. These hfs constants are summarized in Table II. In the presence of DMβ-CyD, the α_{N} value was larger than that in the protic medium, while the α_{H} value was intermediate between those in the protic and aprotic media. These results suggest a configuration of the inclusion complex in which $TPN^{\bullet-}$ penetrates the cavity with its cyano group first at the 3-hydroxyl side and both cyano groups protrude more or less from the CyD cavity.

The large value of α_{N} in the presence of DMβ-CyD greater than that found in a highly protic medium might be unusual. However, this phenomena and also the large values of $K_{\mathrm{red}}/K_{\mathrm{ox}}$ can be considered to arise from a strong dipole–induced dipole interaction between $TPN^{\bullet-}$ and CyD. Because of this interaction, the unpaired π electron appears to be localized on the cyano groups. The (partially) charged cyano groups and the benzene ring moiety seem to be stabilized, respectively, by the solvation with water and hydrophobic interaction with the nonpolar cavity, resulting in the stable inclusion complex formation between $TPN^{\bullet-}$ and CyD.

IPN + CyD Systems. The following electrochemical measurements indicate that IPN and its anion radical ($IPN^{\bullet-}$) are bound with DMβ-CyD, though the formation constants may be much smaller than those of the PN + DBβ-CyD and TPN + DMβ-CyD systems. The addition of 0.05 M DMβ-CyD to an IPN solution reduced the cathodic peak current of an irreversible two-electron reduction by about one-third at $v = 0.1$ V s^{-1}, due to the increase in the apparent diffusion coefficient of IPN by the inclusion complex formation with the CyD, and shifted the cathodic peak potential from −1.866 to −1.790 V vs SCE, suggesting the stronger complex formation of $IPN^{\bullet-}$ relative to IPN. The (quasi) reversible one-electron wave with a midpoint potential of −1.778 V was observed at $v = 60$ V s^{-1} in the presence of 0.05 M DMβ-CyD, but the voltammogram in water remained totally irreversible even at $v = 500$ V s^{-1}.

Similar but weaker effects were observed on the addition of β- and γ-CyDs. The quasi-reversible one-electron wave appeared at $v = 200$ V s^{-1} in the presence of 0.01 M β-CyD or 0.05 M γ-CyD. The addition of 0.05 M α-CyD caused very little change in the voltammogram at $v = 0.1$ V s^{-1}. Hence, we can assume that IPN and $IPN^{\bullet-}$ are incorporated in these CyD cavities in the order of DMβ-CyD > β-CyD > γ-CyD ≫ α-CyD. Steric hindrance between the cyano groups and CyDs may lead to only partial insertion of its benzene ring moiety into the cavities, resulting in the decrease in the formation constant.

In summary, this work has demonstrated that the anion-radical intermediates of dicyanobenzenes, especially $PN^{\bullet-}$ and $TPN^{\bullet-}$, can be strongly included into some CyDs with suitable dimensions and are remarkably stabilized in the local microscopic environment provided by the CyDs. In all cases investigated, the anion radicals are much more strongly bound with CyDs than the parent neutral molecules. Dipole–induced dipole interaction may contribute to increasing the formation constant of the charged guest. However, if a charged guest–CyD inclusion complex has a configuration in which the charge-localized moiety is buried in the hydrophobic CyD cavity, the binding affinity will be decreased. Examples of such complexes are benzoate–α-CyD complex and p-$NP^{\bullet 2-}$–α-CyD complex, where the charged carboxylate or nitro substituent is inserted into the α-CyD cavity.[8,9] Therefore, the direction of penetration and the charge of the guest as well as the dimension of the host all seem to contribute to enhancement of the dipole–induced dipole interaction.

The present study indicates that the interaction between reaction-intermediate radicals of parent guests and CyDs should play an important role in the reaction of the guests under the CyD systems and be taken into consideration in various applications of CyDs. Characterization of the electrochemical and chemical kinetics of the inclusion complexes will be important in fully understanding the role of CyDs.[29] This work suggests also that organic radical intermediates in biological systems could be specifically stabilized in some suitable microscopic environments.

---

(27) The true mechanism would also involve the protonation processes of species B and C in eq 1 and the succeeding reduction processes. In the present analysis based on the simplified mechanism of eq 1, the E_2 value as well as the kinetic fitting parameters (see Experimental Section) should thus be influenced by the above chemical and electrochemical processes. In other words, the E_2 values estimated here have not only thermodynamic but somewhat kinetic nature. Therefore, the present analysis concerning the stability of the included radical is semiquantitative.

(28) Clark, W. M. *Oxidation-Reduction Potentials of Organic Systems*; Williams & Wilkins Co.: Baltimore, 1960; Chapter 4.

(29) Matsue, T.; Evans, D. H.; Osa, T.; Kobayashi, N. *J. Am. Chem. Soc.* **1985**, *107*, 3411.